 CMES, vol.75, no.1, pp.1-31, 2011

A Meshless Hybrid Boundary Node Method for Kirchhoff Plate Bending Problems

F. Tan[1,2], Y.L. Zhang[1], Y.H. Wang[3] and Y. Miao[3]

Abstract: The meshless hybrid boundary node method (HBNM) for solving the bending problem of the Kirchhoff thin plate is presented and discussed in the present paper. In this method, the solution is divided into two parts, i.e. the complementary solution and the particular solution. The particular solution is approximated by the radial basis function (RBF) via dual reciprocity method (DRM), while the complementary one is solved by means of HBNM. The discrete equations of HBNM are obtained from a variational principle using a modified hybrid functional, in which the independent variables are the generalized displacements and generalized tractions on the boundary and the lateral deflection in the domain. The moving least squares (MLS) method is employed to approximate the boundary variables whereas the domain variables are interpolated by a linear combination of fundamental solutions of both the biharmonic equation and Laplace's equation. The present method is a truly boundary type meshless one as it does not require the 'boundary element mesh', either for the purpose of interpolation of the variables or for the integration of 'energy'. Several numerical examples are presented to illustrate the implementation and performance of the present method. It is shown that high accuracy can be achieved with a small node number for clamped and simply supported edge conditions.

Keywords: Meshless method; Hybrid boundary node method; Dual reciprocity method; Plate bending; Kirchhoff Plate.

1 Introduction

The analysis of the plates is a subject of great importance in engineering practice due to the very diffuse employment of these structural members. The thin

[1] State Key Laboratory of Geomechanics and Geotechnical Engineering, Institute of Rock and Soil Mechanics, Chinese Academy of Sciences, Wuhan 430071, China

[2] Corresponding author, Tel: +86-15926324066; Fax: +86-27-87198805; Email: figotan@163.com

[3] School of Civil Engineering and Mechanics, Huazhong University of Science and Technology, Wuhan 430074, China

plate bending problem has been approached by using both analytical and numerical methods. However, realistic problems with complicated geometries and boundary conditions can be solved only numerically. The most popular method is the finite element method (FEM) [Zienkiewic (1977)]. The boundary element method (BEM) has also been applied by many researchers to solve the Kirchhoff plate problem. The first contributions came from Jaswon and Maiti (1968) for plates with smooth boundaries. Further works were proposed by Altiero and Sikarskie (1978), Stern (1979), Paris and Leon (1986, 1987) and by Frangi and Bonnet (1998). More recently Leonetti et al. (2009) proposed a symmetric boundary element model for the analysis of Kirchhoff plates. However, meshing generation required in both of these methods can be a very time-consuming and expensive task.

Compared with the mesh-based methods (e.g. FEM and BEM), meshless methods do not require a mesh, and nodes can be easily added and deleted without a burdensome remeshing. Therefore, meshless methods have been developed rapidly and attracted more and more attention in recent years. According to the way of the discretization, meshless methods can be divided into two categories: the domain type and the boundary type. Several domain type meshless methods, such as the element free Galerkin (EFG) method [Belytchko et al. (1994, 1996)], the point interpolation method (PIM) [Liu and Gu (2001); Leitao (2001); Wang and Liu (2002)] and the meshless local Petrov-Galerkin method (MLPG) [Atluri (2004); Atluri and Shen (2002a, b); Atluri and Zhu (1998, 2000); Gu and Liu (2001); Long and Atluri (2002)] have been proposed and achieved remarkable progress in solving a broad class of boundary value problems.

Based on boundary integral equations, many boundary type meshless methods are developed, such as the local boundary integral equation (LBIE) method [Atluri et al. (2000); Sladek et al. (2002); Zhu et al. (1998)], the boundary node method (BNM) [Kothnur et al. (1999); Mukherjee and Mukherjee (1997a)], the boundary particle method (BPM) [Fu and Chen (2009)], the boundary element free method (BEFM) [Kitipornchai et al. (2005); Liew et al. (2006)] and the Galerkin boundary node method (GBNM) [Li and Zhu (2009, 2011)]. Compared with the domain type meshless methods, these methods require only a nodal data structure on the boundary surface of a body whose dimension is one less than that of the domain itself.

The aforementioned meshless methods do not need an element mesh for the interpolation of the field or boundary variables, but some of them have to use background cells for integration. The requirement of background cells for integration makes the methods being not 'truly' meshless.

Zhang and Yao (2001, 2004) proposed another boundary type meshless method: the hybrid boundary node method (HBNM). The HBNM gets rid of the background el-

ements and is a truly boundary type meshless method. It employs the moving least squares (MLS) [Lancaster and Salkauskas (1981)] to approximate the boundary variables, and the integration is limited to a fixed local region on the boundary. No elements are needed either for interpolation or for integration, and at the same time it has the advantage of dimensionality reduction. This method has been employed to solve the potential problems [Zhang and Yao (2001); Zhang et al. (2002)], and the elastostatics problems [Zhang and Yao (2004); Miao et al. (2005)]. Like the BEM, it is not convenient for solving elastodynamics analysis because applying the elastodynamics fundamental solution increases the computational effort and the domain integration is inevitable. To overcome these drawbacks, the dual reciprocity method (DRM) [Patridge et al. (1992)] was introduced into HBNM by Miao et al. (2009) and Yan et al. (2009), and a new truly meshless method Dual Hybrid Boundary Node Method (DHBNM) is proposed. However, for the thin plate bending problems, the governing equation is the fourth order PDE, which makes it difficult to employ the DHBNM directly.

In this paper, the dual hybrid boundary node method will be developed for solving the bending problem of a thin plate. The solutions in this method are divided into two parts: complementary solution and particular solution. For the particular solution, DRM has been used and the radial basis functions are applied to interpolating the inhomogeneous parts of the equations, i.e. the distributed load per unit area normal to the plate, while the complementary one is solved by means of HBNM. The discrete equations of HBNM are obtained from a variational principle using a modified hybrid functional which is expressed in terms of five independent variables. On the boundary these variables are the generalized displacements, i.e. deflection and normal slope, and the generalized tractions, i.e. normal bending and effective shear force per unit length. In the domain the functional involves the deflection only. In this approach, the boundary variables are approximated using MLS, whereas the domain variables are interpolated by a linear combination of fundamental solutions of both the biharmonic equation and Laplace's equation. Numerical examples presented in the present paper for the solution of thin plate bending problems demonstrate the validity and accuracy of the proposed approach.

The following discussions begin with the brief description of the Kirchhoff plate bending theory in Section 2. The DHBNM for thin plate bending problems is developed in Section 3. Some numerical examples for thin plates having different boundary conditions are shown in Section 4. Finally, the paper ends with conclusions in Section 5.

2 Kirchhoff plate bending theory

A thin plate, defined over the domain Ωdelimited by the boundaryΓ, is considered (Fig. 1). In the Kirchhoff theory the assumption of negligible shear deformations lead to the description of the plate bending only in terms of the transversal displacement $w(x,y)$ [Timoshenko and Woinowsky-Krieger (1959)]. The governing equation is

$$D\nabla^4 w = p \tag{1}$$

where w is the deflection of the middle surface of the plate, p is the prescribed distributed load per unit area normal to the plate, ∇^4 is the biharmonic operator, and D is the flexural rigidity being given as(E is the elastic modulus, μ is the Poisson coefficient and t is the plate thickness)

$$D = \frac{Et^3}{12(1-\mu^2)}$$

The following general form of boundary conditions is considered:

$$\begin{cases} w = \bar{w} & \forall x \in \Gamma_w \\ \theta_n = \bar{\theta}_n & \forall x \in \Gamma_\theta \end{cases} \tag{2}$$

$$\begin{cases} M_{nn} = \bar{M}_{nn} & \forall x \in \Gamma_M \\ V_n = \bar{V}_n & \forall x \in \Gamma_V \end{cases} \tag{3}$$

where θ_n, M_{nn} and $V_n$denote the normal slope, bending moment and effective shear force, respectively. The barred symbols denote prescribed boundary values.

The Eqs. (2)-(3) may also be expressed in terms of the deflection $w$as follows

Normal slope:

$$\theta_n = \frac{\partial w}{\partial n} = w_{,i} n_i \tag{4}$$

Normal bending moment and twist moment:

$$M_{nn} = -D[\mu w_{,ii} + (1-\mu) w_{,ij} n_i n_j] \tag{5}$$

$$M_{nt} = -D(1-\mu) w_{,ij} n_i t_j \tag{6}$$

Normal shear force and effective shear force:

$$Q_n = -D w_{,ijj} n_i \tag{7}$$

$$V_n = Q_n + \frac{\partial M_{nt}}{\partial s} = -D[w_{,ijj}n_i + (1-\mu)(w_{,ijk}n_i t_j t_k + \rho^{-1} w_{,ij} t_i t_j - \rho^{-1} w_{,ij} n_i n_j)] \quad (8)$$

where $\mathbf{n} = [n_1, n_2]$ and $\mathbf{t} = [t_1, t_2]$ are the unit normal vector and tangential vector to the boundary Γ, respectively; s is the arc length along the boundary; ρ is the radius of curvature, with $\rho^{-1} = 0$ along a straight line boundary.

At any regular point of the boundary, two such boundary conditions must be assigned. For any well-posed boundary value problem,$\Gamma_w \cap \Gamma_V = 0$, $\Gamma_w \cup \Gamma_V = \Gamma$ and $\Gamma_\theta \cap \Gamma_M = 0$, $\Gamma_\theta \cup \Gamma_M = \Gamma$. Additionally, there are two kinds of boundary conditions for some corner points:

$$w_{k_1} = \bar{w}_{k_1} \quad (k_1 = 1, 2, \cdots, k_w) \quad (9)$$

$$\|M_{nt}\|_{k_2} = \|\bar{M}_{nt}\|_{k2} \quad (k_2 = 1, 2, \cdots, k_p) \quad (10)$$

where k_w is the number of corner points which the deflections are prescribed, k_p is the number of corner points which the concentrated forces are prescribed and $\|M_{nt}\|$denotes the fictitious corner force due to the jump of discontinuity of the twist moment.

The boundary conditions that usually appear along the boundary are:

simply supported edge:

$$w = \bar{w}; \quad M_{nn} = \bar{M}_{nn} \quad (11)$$

clamped edge:

$$w = \bar{w}; \quad \theta_n = \bar{\theta}_n \quad (12)$$

free edge:

$$M_{nn} = \bar{M}_{nn}; \quad V_n = \bar{V}_n \quad (13)$$

3 Dual hybrid boundary node method for solving the bending problem of a thin plate

In this paper, the solution variable w can be divided into complementary solution w^c and particular solution w^p, i.e.

$$w = w^c + w^p \quad (14)$$

The particular solution w^p just needs to satisfy the inhomogeneous equation as follows:

$$D\nabla^4 w^p = p \quad (15)$$

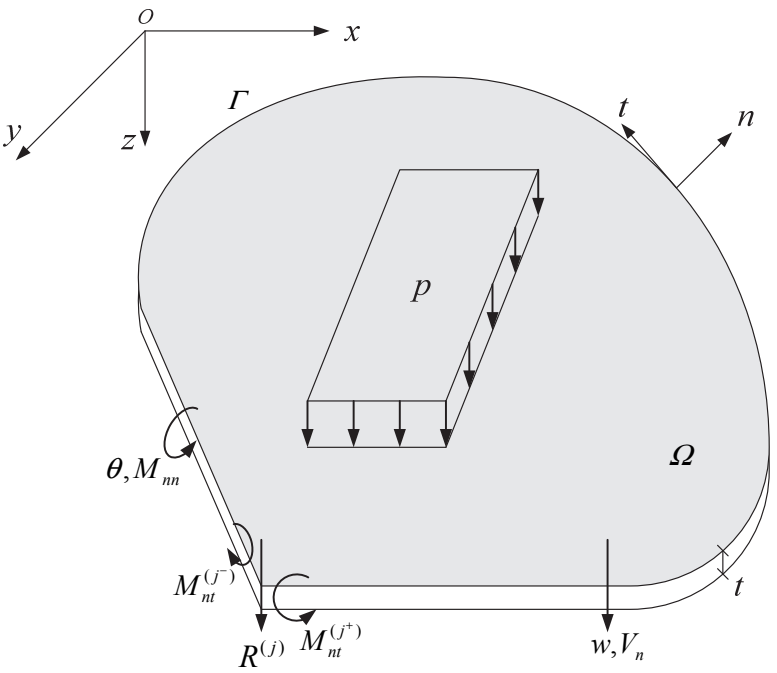

Figure 1: Variables of Kirchhoff plate model

And the complementary solution w^c has to satisfy the biharmonic equation and the modified boundary condition, i.e.

$$D\nabla^4 w^c = 0 \tag{16}$$

$$\begin{cases} w^c = \bar{w}^c = \bar{w} - w^p & \forall x \in \Gamma_w \\ \theta_n^c = \bar{\theta}_n^c = \bar{\theta}_n - \theta_n^p & \forall x \in \Gamma_\theta \end{cases} \tag{17}$$

$$\begin{cases} M_{nn}^c = \bar{M}_{nn}^c = \bar{M}_{nn} - M_{nn}^p & \forall x \in \Gamma_M \\ V_n^c = \bar{V}_n^c = \bar{V}_n - V_n^p & \forall x \in \Gamma_V \end{cases} \tag{18}$$

3.1 Dual reciprocity method

The DRM can be used in thin plate bending problem to transform the domain integral arising from the transversal load term into the equivalent boundary integrals. Applying interpolation for inhomogeneous term, the following approximation can

be proposed for the term p in Eq. (1) [Patridge et al. (1992)]

$$p \approx \sum_{j=1}^{N+L} f^j \alpha^j \tag{19}$$

where f^j are the approximation functions, α^j are a set of initially unknown coefficients, N and L are the total number of the boundary nodes and total number of interior nodes, respectively.

The particular solution w^p can be written as follows

$$w^p = \sum_{j=1}^{N+L} \alpha^j \hat{w}^j \tag{20}$$

where $\hat{w}^j$ satisfies following equation

$$D\nabla^4 \hat{w}^j = f^j \tag{21}$$

The approximation function, f^j, can be chosen as $f^j = 1 + r$. Obviously, the particular solution $\hat{w}^j$ satisfying Eq.(21) can be obtained as

$$\hat{w}^j = \frac{1}{D}\left(\frac{1}{64} r^4 + \frac{1}{225} r^5\right) \tag{22}$$

The corresponding expressions for the normal slope $\hat{\theta}^j$, bending moment $\hat{M}^j$ and effective shear force $\hat{V}^j$ can be obtained by Eqs. (4), (5) and (8). Solving Eq. (19), one can obtain the particular solution in matrix form as

$$\mathbf{w^p} = \hat{\mathbf{W}}\mathbf{F}^{-1}\mathbf{p} \tag{23}$$

$$\theta_{\mathbf{n}}^{\mathbf{p}} = \hat{\mathbf{\Theta}}\mathbf{F}^{-1}\mathbf{p} \tag{24}$$

$$\mathbf{M_{nn}^p} = \hat{\mathbf{M}}\mathbf{F}^{-1}\mathbf{p} \tag{25}$$

$$\mathbf{V_n^p} = \hat{\mathbf{V}}\mathbf{F}^{-1}\mathbf{p} \tag{26}$$

where vector $\mathbf{p}$ is the value of transversal load on each node, each column of $\mathbf{F}$ consists of a vector f^j containing the values of the function f^j at the DRM collocation nodes, and $\hat{\mathbf{W}}$, $\hat{\mathbf{\Theta}}$, $\hat{\mathbf{M}}$ and $\hat{\mathbf{V}}$ are the matrix forms of the basis type of particular solutions.

3.2 Development of the hybrid boundary node method

3.2.1 Variational principle

The total potential energy can be given as

$$\Pi_p = \int_\Omega \frac{1}{2} D_{ijkl} w_{,ij} w_{,kl} \, \mathrm{d}\Omega - \int_\Omega p w \, \mathrm{d}\Omega + \int_{\Gamma_M} \bar{M}_{nn} \theta_n \, \mathrm{d}\Omega - \int_{\Gamma_V} \bar{V}_n w \, \mathrm{d}\Gamma - \sum_{k_1=1}^{k_p} \left\| M_{nt} \right\|_{k_1} w_{k_1} \quad (27)$$

where D_{ijkl} is the matrix of the flexural rigidity. For the isotropic elastic thin plates,

$$D_{ijkl} = D\mu \delta_{ij} \delta_{kl} + D(1-\mu) \delta_{il} \delta_{jk} \quad (28)$$

In this paper, the HBNM is based on a modified variational principle. For thin plate problems, the functions to be independent are: deflection of the plate in the domain, w; generalized displacement on the boundary, i.e. deflection, $\tilde{w}$ and normal slope, $\tilde{\theta}_n$; generalized tractions on the boundary, i.e. normal bending, $\tilde{M}_{nn}$ and effective shear force, $\tilde{V}_n$.

The modified variational functional is defined as

$$\Pi_p^* = \Pi_p - \int_\Gamma (w - \tilde{w}) \tilde{V}_n \, \mathrm{d}\Omega + \int_\Gamma (\theta_n - \tilde{\theta}_n) \tilde{M}_{nn} \, \mathrm{d}\Omega + \sum_{k_2=1}^{k_w} (w_{k_2} - \tilde{w}_{k_2}) \left\| \tilde{M}_{nt} \right\|_{k_2} \quad (29)$$

For the complementary solution, Eq. (18) is satisfied where the inhomogeneous term $p = 0$. And taking the variational of Eq. (29), we have

$$\begin{aligned} \delta \Pi_p^* = & \int_\Omega D w_{,iijj} \delta w \, \mathrm{d}\Omega + \int_\Gamma (V_n - \tilde{V}_n) \, \delta w \, \mathrm{d}\Gamma \\ & - \int_\Gamma (M_{nn} - \tilde{M}_{nn}) \, \delta \theta_n \, \mathrm{d}\Gamma + \int_\Gamma (\theta_n - \tilde{\theta}_n) \, \delta \tilde{M}_{nn} \, \mathrm{d}\Gamma - \int_\Gamma (w - \tilde{w}) \, \delta \tilde{V}_n \, \mathrm{d}\Gamma \\ & - \int_{\Gamma_M} (\tilde{M}_{nn} - \bar{M}_{nn}) \, \delta \theta_n \mathrm{d}\Gamma + \int_{\Gamma_V} (\tilde{V}_n - \bar{V}_n) \, \delta w \, \mathrm{d}\Gamma \\ & - \sum_{k_2=1}^{k_p} (\left\| M_{nt} \right\|_{k_2} - \left\| \bar{M}_{nt} \right\|_{k_2}) \, \delta w_{k_2} + \sum_{k_1=1}^{k_w} (w_{k_1} - \tilde{w}_{k_1}) \, \delta \left\| \tilde{M}_{nt} \right\|_{k_1} \end{aligned} \quad (30)$$

Let $\delta \Pi_p^* = 0$, the following integration equations can be obtained as

$$\int_\Omega D w_{,iijj} \delta w \, \mathrm{d}\Omega + \int_\Gamma (V_n - \tilde{V}_n) \, \delta w \, \mathrm{d}\Gamma = 0 \quad (31)$$

$$\int_{\Gamma} (M_{nn} - \tilde{M}_{nn})\, \delta\theta_n \, \mathrm{d}\Gamma = 0 \tag{32}$$

$$\int_{\Gamma} (\theta_n - \tilde{\theta}_n)\, \delta\tilde{M}_{nn} \, \mathrm{d}\Gamma = 0 \tag{33}$$

$$\int_{\Gamma} (w - \tilde{w})\, \delta\tilde{V}_n \, \mathrm{d}\Gamma = 0 \tag{34}$$

$$\int_{\Gamma_M} (\tilde{M}_{nn} - \bar{M}_{nn})\, \delta\theta_n \, \mathrm{d}\Gamma = 0 \tag{35}$$

$$\int_{\Gamma_V} (\tilde{V}_n - \bar{V}_n)\, \delta w \, \mathrm{d}\Gamma = 0 \tag{36}$$

$$\sum_{k_2=1}^{k_p} (\|M_{nt}\|_{k_2} - \|\bar{M}_{nt}\|_{k_2})\, \delta w_{k_2} = 0 \tag{37}$$

$$\sum_{k_1=1}^{k_w} (w_{k_1} - \tilde{w}_{k_1})\, \delta \left\|\tilde{M}_{nt}\right\|_{k_1} = 0 \tag{38}$$

If the generalized traction boundary condition and the corner points conditions are imposed, Eqs. (35)-(38) will be satisfied and they would be ignored in the following analysis.

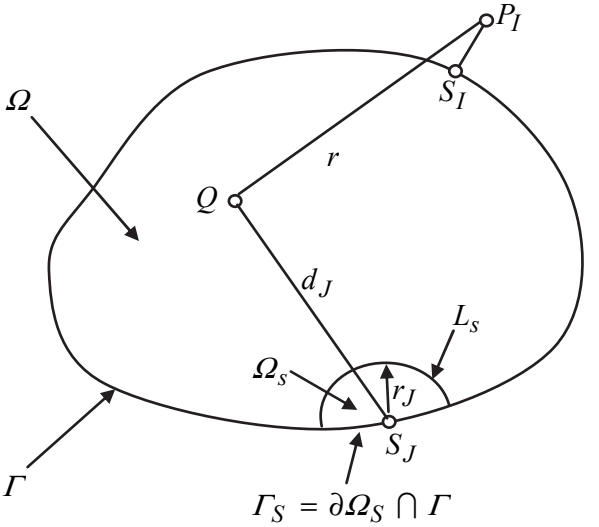

Figure 2: Local domain centered at node s_J and source point of fundamental solution corresponding to node s_I

It can be seen that Eqs. (31)-(34) hold for any portion of the domain Ω, for example, in a sub-domain Ω_s, which is bounded by Γ_s and L_s (Fig. 2). Following Refs. [Atluri and Zhu (1998)], the weak forms on a sub-domain Ω_s and its boundaries Γ_s and L_s are used to replace Ω and Γ in Eqs. (31)-(34). The test function $v_J(Q)$ is used to replace the variational part. They can be presented as

$$\int_{\Omega_s} Dw_{,iijj}\, v\, \mathrm{d}\Omega + \int_{\Gamma_s+L_s} (V_n - \tilde{V}_n)\, v\, \mathrm{d}\Gamma = 0 \tag{39}$$

$$\int_{\Gamma_s+L_s} (M_{nn} - \tilde{M}_{nn})\, v\, \mathrm{d}\Gamma = 0 \tag{40}$$

$$\int_{\Gamma_s+L_s} (\theta_n - \tilde{\theta}_n)\, v\, \mathrm{d}\Gamma = 0 \tag{41}$$

$$\int_{\Gamma_s+L_s} (w - \tilde{w})\, v\, \mathrm{d}\Gamma = 0 \tag{42}$$

In Eqs. (39)-(42), the variable of $\tilde{w}$, $\tilde{\theta}_n$, $\tilde{M}_{nn}$ and $\tilde{V}_n$ on L_s are not defined. If $v_J(Q)$ can be selected in such a way that the integral over L_s vanishes, the problem can be solved conveniently. Thus the sub-domain Ω_s is chosen as the intersection of the domain Ω and a circle centered at a boundary node, s_J (Fig. 2), and the test function $v_J(Q)$ can be written in the form

$$v_J(Q) = \begin{cases} \frac{\exp[-(d_J/c_J)^2] - \exp[-(r_J/c_J)^2]}{1 - \exp[-(r_J/c_J)^2]} & 0 \le d_J \le r_J \\ 0 & d_J \ge r_J \end{cases} \tag{43}$$

where d_J is the distance between the integral point Q in the domain and the nodal point s_J; c_J is a constant controlling the test function shape, and r_J is the radius of the sub-domain. From Eq. (43) it can be seen that $v_J(Q)$ vanishes on the boundary L_S. Therefore, Eqs. (39)-(42) can be rewritten as follows

$$\int_{\Omega_s} Dw_{,iijj}\, v\, \mathrm{d}\Omega + \int_{\Gamma_s} (V_n - \tilde{V}_n)\, v\, \mathrm{d}\Gamma = 0 \tag{44}$$

$$\int_{\Gamma_s} (M_{nn} - \tilde{M}_{nn})\, v\, \mathrm{d}\Gamma = 0 \tag{45}$$

$$\int_{\Gamma_s} (\theta_n - \tilde{\theta}_n)\, v\, \mathrm{d}\Gamma = 0 \tag{46}$$

$$\int_{\Gamma_s} (w - \tilde{w})\, v\, \mathrm{d}\Gamma = 0 \tag{47}$$

3.2.2 Variables interpolation

As a truly boundary-type meshless method, the HBNM uses the MLS to approximate the boundary variables, and applies the fundamental solution interpolation to obtain the solutions in the domain.

By using the MLS principle, the boundary variables$\tilde{w}$, $\tilde{\theta}_n$, $\tilde{M}_{nn}$ and $\tilde{V}_n$ can be written as

$$\tilde{w} = \sum_{I=1}^{N} \Phi_I \check{w}_I \tag{48}$$

$$\tilde{\theta}_n = \sum_{I=1}^{N} \Phi_I \check{\theta}_I \tag{49}$$

$$\tilde{M}_{nn} = \sum_{I=1}^{N} \Phi_I \check{M}_I \tag{50}$$

$$\tilde{V}_n = \sum_{I=1}^{N} \Phi_I \check{V}_I \tag{51}$$

where N stands for the number of nodes located on the boundary; $\check{w}_I$, $\check{\theta}_I$, $\check{M}_I$ and $\check{V}_I$ are the fictitious nodal values; Φ_I is the shape function of the MLS, which is given by

$$\Phi_I(s) = \sum_{j=1}^{m} p_j(s) \left[A^{-1}(s) B(s)\right]_{jI} \tag{52}$$

In the above equation, s is a curvilinear coordinate, $p_j(s)$ provide a basis function of order m. In this study, m is taken as 3, i.e., $\mathbf{p}^{\mathrm{T}}(s) = [1, s, s^2]$. Matrices $\mathbf{A}(s)$ and $\mathbf{B}(s)$ are defined as

$$\mathbf{A}(s) = \mathbf{p}^{\mathrm{T}}(s)\, \mathbf{w}(s)\, \mathbf{p}(s) \tag{53}$$

$$\mathbf{B}(s) = \mathbf{p}^{\mathrm{T}}(s)\, \mathbf{w}(s) \tag{54}$$

In Eqs. (53) and (54), $\mathbf{w}(s)$ is the weight matrix. This is a diagonal matrix where the diagonal elements are$w_I(s)$. In the study, the Gaussian weight function is chosen and can be written as

$$w_I(s) = \begin{cases} \frac{\exp[-(d_I/c_I)^2] - \exp[-(\hat{d}_I/c_I)^2]}{1 - \exp[-(\hat{d}_I/c_I)^2]} & 0 \le d_I \le \hat{d}_I \\ 0 & d_I \ge \hat{d}_I \end{cases} \tag{55}$$

where $d_I = |s - s_I|$ is the distance between an evaluation point and node s_I; c_I is a constant controlling the shape of the weight function $w_I(s)$; $\hat{d}_I$ is the size of the support for the weight function $w_I(s)$ and determines the support of node s_I.

For the thin plate bending problems, the domain variables$w$,θ_n,M_{nn} and V_n are interpolated by a linear combination of the fundamental solutions of both the biharmonic equation and Laplace's equation. They can be written as

$$w = \sum_{I=1}^{N} (w_1^I x_1^I + w_2^I x_2^I) \tag{56}$$

$$\theta_n = \sum_{I=1}^{N} (\theta_1^I x_1^I + \theta_2^I x_2^I) \tag{57}$$

$$M_{nn} = \sum_{I=1}^{N} (M_1^I x_1^I + M_2^I x_2^I) \tag{58}$$

$$V_n = \sum_{I=1}^{N} (V_1^I x_1^I + V_2^I x_2^I) \tag{59}$$

where w_1^I is the fundamental solution of the biharmonic equation and w_2^I is the fundamental solution of the Laplace's equation; x_1^I and x_2^I are unknown parameters. The fundamental solutions are written as

$$w_1^I = -\frac{1}{8\pi D} r^2 \ln r \tag{60}$$

$$w_2^I = -\frac{1}{2\pi D} \ln r \tag{61}$$

where $r = r(Q, P_I) = \sqrt{(x(Q) - x(P_I))^2 + (y(Q) - y(P_I))^2}$; Q and P_I are the field point and source point, respectively. And P_I is determined by

$$P_I = S_I + h\,\xi\, n(S_I) \tag{62}$$

where h is the mesh size; $n(S_I)$ is the outward normal direction to the boundary at node S_I; ξ is the scale factor and plays an important role in the performance of the present method.

Substituting the Eqs. (60) and (61) into Eqs. (4), (5) and (8), one can obtain the corresponding expressions for θ_1^I, θ_2^I, M_1^I, M_2^I, V_1^I and V_2^I.

As w is expressed by Eq. (56), the term $w_{,iijj}$ in the left hand of Eq. (44) vanished. By substituting Eqs. (48)-(51), (58)-(59) into Eqs. (44)-(47), and omitting the vanished terms, we have

$$\sum_{I=1}^{N}\int_{\Gamma_s}\begin{bmatrix}V_1^I & V_2^I\end{bmatrix}\begin{Bmatrix}x_1^I\\ x_2^I\end{Bmatrix}v_J(Q)\,\mathrm{d}\Gamma=\sum_{I=1}^{N}\int_{\Gamma_s}\Phi_I\check{V}_I v_J(Q)\,\mathrm{d}\Gamma \tag{63}$$

$$\sum_{I=1}^{N}\int_{\Gamma_s}\begin{bmatrix}M_1^I & M_2^I\end{bmatrix}\begin{Bmatrix}x_1^I\\ x_2^I\end{Bmatrix}v_J(Q)\,\mathrm{d}\Gamma=\sum_{I=1}^{N}\int_{\Gamma_s}\Phi_I\check{M}_I v_J(Q)\,\mathrm{d}\Gamma \tag{64}$$

$$\sum_{I=1}^{N}\int_{\Gamma_s}\begin{bmatrix}\theta_1^I & \theta_2^I\end{bmatrix}\begin{Bmatrix}x_1^I\\ x_2^I\end{Bmatrix}v_J(Q)\,\mathrm{d}\Gamma=\sum_{I=1}^{N}\int_{\Gamma_s}\Phi_I\check{\theta}_I v_J(Q)\,\mathrm{d}\Gamma \tag{65}$$

$$\sum_{I=1}^{N}\int_{\Gamma_s}\begin{bmatrix}w_1^I & w_2^I\end{bmatrix}\begin{Bmatrix}x_1^I\\ x_2^I\end{Bmatrix}v_J(Q)\,\mathrm{d}\Gamma=\sum_{I=1}^{N}\int_{\Gamma_s}\Phi_I\check{w}_I v_J(Q)\,\mathrm{d}\Gamma \tag{66}$$

Using the above equations for all nodes, one can get the system equations

$$\mathbf{V}\mathbf{x}=\mathbf{H}\check{\mathbf{V}}^c \tag{67}$$

$$\mathbf{M}\mathbf{x}=\mathbf{H}\check{\mathbf{M}}^c \tag{68}$$

$$\mathbf{\Theta}\mathbf{x}=\mathbf{H}\check{\theta}^c \tag{69}$$

$$\mathbf{W}\mathbf{x}=\mathbf{H}\check{\mathbf{w}}^c \tag{70}$$

where

$$V_{IJ}=\int_{\Gamma_s^I}\begin{bmatrix}V_1^J & V_2^J\end{bmatrix}v_I(Q)\,\mathrm{d}\Gamma$$

$$H_{IJ}=\int_{\Gamma_s^I}\Phi_J v_I(Q)\,\mathrm{d}\Gamma$$

$$M_{IJ}=\int_{\Gamma_s^I}\begin{bmatrix}M_1^J & M_2^J\end{bmatrix}v_I(Q)\,\mathrm{d}\Gamma$$

$$\Theta_{IJ}=\int_{\Gamma_s^I}\begin{bmatrix}\theta_1^J & \theta_2^J\end{bmatrix}v_I(Q)\,\mathrm{d}\Gamma$$

$$W_{IJ} = \int_{\Gamma_s^I} \begin{bmatrix} w_1^J & w_2^J \end{bmatrix} v_I(Q)\, \mathrm{d}\Gamma$$

$$\mathbf{x} = [x_1^1, x_1^2, \cdots, x_1^N, x_1^N]^{\mathrm{T}}$$

$$\check{\mathbf{V}}^{\mathrm{c}} = [\check{V}_1, \check{V}_2, \cdots, \check{V}_N]^{\mathrm{T}}$$

$$\check{\mathbf{M}}^{\mathrm{c}} = [\check{M}_1, \check{M}_2, \cdots, \check{M}_N]^{\mathrm{T}}$$

$$\boldsymbol{\theta}^{\mathrm{c}} = [\check{\theta}_1, \check{\theta}_2, \cdots, \check{\theta}_N]^{\mathrm{T}}$$

$$\check{\mathbf{w}}^{\mathrm{c}} = [\check{w}_1, \check{w}_2, \cdots, \check{w}_N]^{\mathrm{T}}$$

The evaluation of the matrices $\mathbf{V}$, $\mathbf{M}$, $\boldsymbol{\Theta}$ and $\mathbf{W}$ is much simpler in this approach than in BEM and BNM. No singular integrations are involved, because the source points of the fundamental solutions are located at a distance from the boundary of the domain.

3.3 Dual hybrid boundary node method

In the DHBNM, the MLS approximation is employed to construct the shape function. However, same as the EFG method, there is an issue of imposition of the essential boundary conditions [Mukherjee and Mukherjee (1997b); Zhu and Atluri (1998)].

For a well-posed problem, there should be two prescribed boundary values at each node on the boundary. The corresponding fictitious nodal values $\check{w}_I$, $\check{\theta}_I$,$\check{M}_I$ and $\check{V}_I$ can be obtained as follows

$$\check{w}_I = \sum_{J=1}^{N} R_{IJ} \bar{w}_{cJ} \tag{71}$$

$$\check{\theta}_I = \sum_{J=1}^{N} R_{IJ}\bar{\theta}_{cJ} \tag{72}$$

$$\check{M}_I = \sum_{J=1}^{N} R_{IJ}\bar{M}_{cJ} \tag{73}$$

$$\check{V}_I = \sum_{J=1}^{N} R_{IJ}\bar{V}_{cJ} \tag{74}$$

where $R_{IJ} = \left[\Phi_J\left(s_I\right)\right]^{-1}$, and $\bar{w}_{cJ}$, $\bar{\theta}_{cJ}$, $\bar{M}_{cJ}$ and $\bar{V}_{cJ}$ are the complementary solutions of boundary node J.

Substituting Eqs. (23)-(26), (71)-(74) into Eq. (14), then substitute the result into Eqs. (67)-(70), we can obtain

$$\mathbf{Vx} + \mathbf{HR}\hat{\mathbf{V}}\mathbf{F}^{-1}\mathbf{p} = \mathbf{HV_n} \tag{75}$$

$$\mathbf{Mx} + \mathbf{HR}\hat{\mathbf{M}}\mathbf{F}^{-1}\mathbf{p} = \mathbf{HM_{nn}} \tag{76}$$

$$\boldsymbol{\Theta}\mathbf{x} + \mathbf{HR}\hat{\boldsymbol{\Theta}}\mathbf{F}^{-1}\mathbf{p} = \mathbf{HR}\boldsymbol{\theta}_\mathbf{n} \tag{77}$$

$$\mathbf{Wx} + \mathbf{HR}\hat{\mathbf{W}}\mathbf{F}^{-1}\mathbf{p} = \mathbf{HRw} \tag{78}$$

The number of unknown vector $\mathbf{x}$ is $2N$. One can choose $2N$ equations from Eqs. (75)-(78) which the boundary conditions are prescribed, rearrange them, and obtain $2N$ system equations in term of $\mathbf{x}$ only. The unknown vector $\mathbf{x}$ can be obtained by solving the final system equations.

From the above derivation procedure, it can be seen that the present method is a truly meshless method, as absolutely no boundary elements are needed, either for the interpolation purpose or for the integration purpose. The points inside the domain are needed just for the particular solution interpolation, which can not deny the present method being a boundary type method. Besides, there is no singular integral in the method, and no further integration is needed in the 'post-processing' step.

4 Numerical examples

In this section, some numerical examples are presented to show the accuracy and the efficiency of the proposed method. The parameters that influence the performance of the method are also investigated. The results of the present method are compared with the analytical solutions or the results obtained by others numerical methods (e.g. BEM or FEM).

In all the following examples, the support size for the weight function $\hat{d}_I$ in Eq. (55) is taken to be $3.5h$, and the corresponding parameter c_I is taken to be such that $\hat{d}_I/c_I = 4.0$. The radius of the sub-domain r_J in Eq. (43) is chosen as $0.8h$, and the parameter c_J is taken to be such that $r_J/c_J = 1.2$. The scale factor $\xi = 6.0$ in Eq. (62). Also, in all integrations, five Gauss points are used on each part of the two sections of Γ_s. In order to deal with the discontinuities at the corners, the nodes are not arranged at these places and the support domain for interpolation is truncated. The material properties are: $E = 2.1 \times 10^{10}$Pa, $\mu = 0.3$ and $t = 0.1$m.

4.1 A simply supported equilateral triangular plate

This example consists of analyzing a simply supported equilateral triangular plate subjected to a constant normal moment along all edges (see Fig. 3).

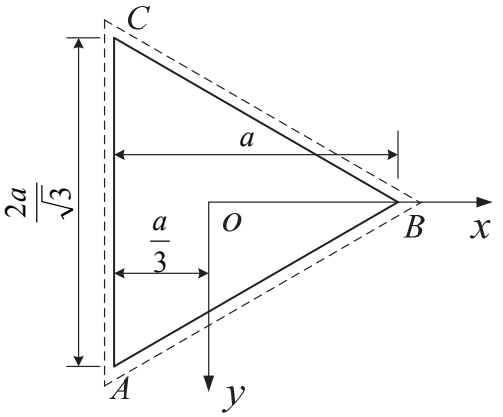

Figure 3: A simply-supported equilateral triangular plate loaded by moments M_{nn} uniformly distributed along the boundary

In this case, $a = 3$m and $M_{nn} = 500\text{m} \cdot \text{N / m}$, and the analytical expression of the deflection surface is [Timoshenko and Woinowsky-Krieger (1959)]:

$$w = \frac{M_{nn}}{4aD}\left[x^3 - 3y^2x - a\left(x^2+y^2\right) + \frac{4}{27}a^3\right] \tag{79}$$

In the present calculation, three different nodes arrangements of 5, 10 and 20 nodes on each edge are used to study the convergence of the present method. Because the

plate is loaded by normal moments M_{nn} uniformly distributed along the boundary, i.e. $p = 0$ and no internal points are required in DRM. The numerical results for five points inside the domain are listed in Table 1 where 10 nodes on each edge are used, and they are compared with the analytical solutions. Fig. 4 shows the distribution of normal slope θ_n along the boundary AC. It can be seen that the good accuracy is achieved even with a few nodes.

Table 1: Deflections, bending moments and their relative error inside the domain

Location	Deflection $w(\times D)$			Bending moment M_x		
	Numerical solution	Analytical solution	Relative error (%)	Numerical solution	Analytical solution	Relative error (%)
(-0.5, 0.0)	130.213142	130.2083	0.0037	499.9621	500.0	0.0025
(0.0, 0.0)	166.672478	166.6667	0.0035	412.4897	412.5	0.0024
(0.5, 0.0)	140.629667	140.625	0.0033	325.0078	325.0	0.0054
(1.0, 0.0)	83.334176	83.33334	0.0010	237.5129	237.5	0.0323
(1.5, 0.0)	26.051783	26.04167	0.0388	149.9515	150.0	0.1454

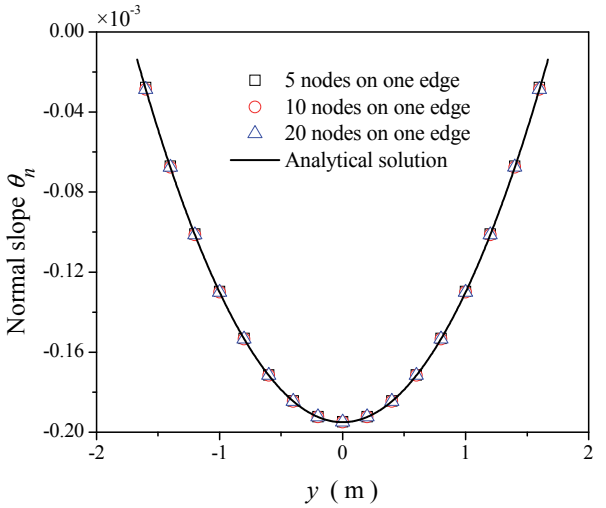

Figure 4: Normal slope θ_n along the boundary AC

The relative errors of the deflection$w$ and bending moment M_{xx} at the central point O with different scale factor ξ are shown in Fig. 5. It can be seen that the results are all very accurate when$\xi \geq 2.0$, and the numerical results of deflection w are

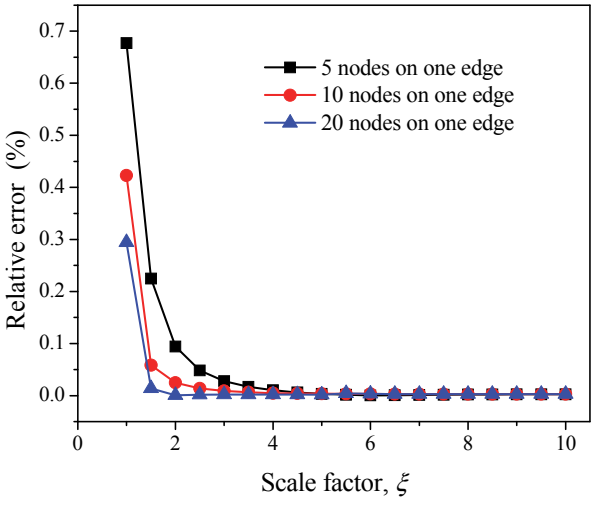

(a) Relative error of the deflection w

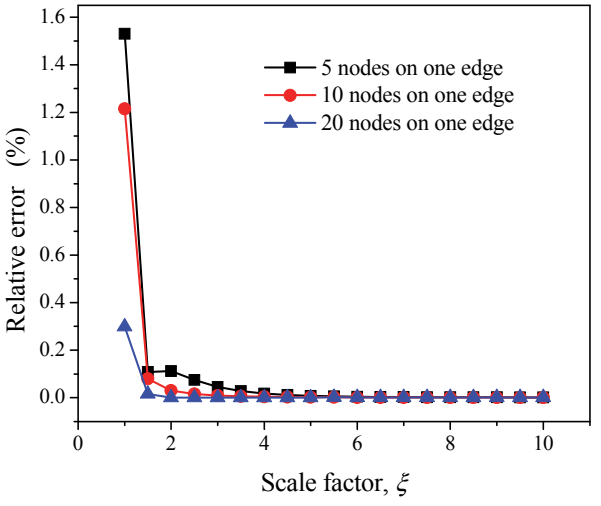

(b) Relative error of the bending moment M_{xx}

Figure 5: Relative error at the central point O with different scale factor ξ for the simply supported equilateral triangular plate

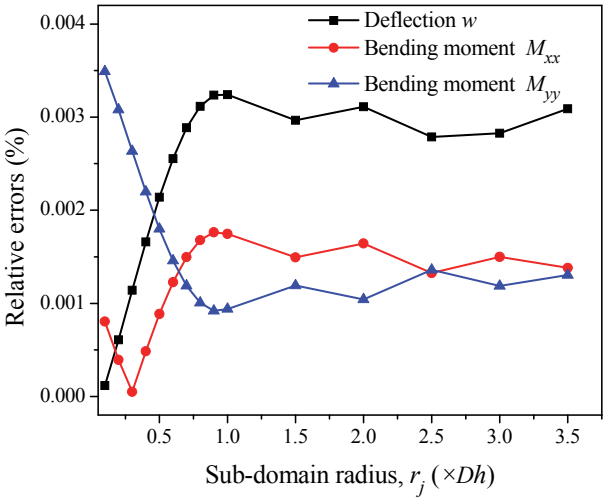

Figure 6: Relative error at the central point O with different sub-domain radius r_j for the simply supported equilateral triangular plate

more accurate than bending moment M_{xx}. However, too large value of ξ will lead to ill-conditioned equations. Actually, further computations of this example show that the biggest value of ξ which ensures that the present method is non-degenerate is 20.0, and this value is independent of the boundary conditions while dependent on the domain geometry and meshing.

The influence of the sub-domain radius r_j is also examined. Fig. 6 shows the relative errors of w, M_{xx} and M_{yy}at the central point O with different sub-domain radius r_j. It should be noted that $\cup\Gamma_s$do not cover the whole bounding surface when $r_j < 0.5h$, and will be overlapped when $r_j \geq 0.5h$. It is shown that the results are in all cases accurate regardless that Γ_s are overlapped, or even uncover the whole boundary.

4.2 Circle plate

A circular plate of radius a carries a load of intensity q uniformly distributed over the entire surface of the plate (see Fig. 7). Because the load is symmetrically distributed about the axis perpendicular to the plate through its center, the deflection surface will also be symmetrical.

For the circular plate with clamped edges, the analytical solution of the deflection

at a distance r from the center is [Timoshenko and Woinowsky-Krieger (1959)]:

$$w = \frac{q}{64D}\left(a^2 - r^2\right)^2 \tag{80}$$

For the circular plate with supported edges, the analytical solution is [Timoshenko and Woinowsky-Krieger (1959)]:

$$w = \frac{q\left(a^2 - r^2\right)}{64D}\left(\frac{5+\mu}{1+\mu}a^2 - r^2\right) \tag{81}$$

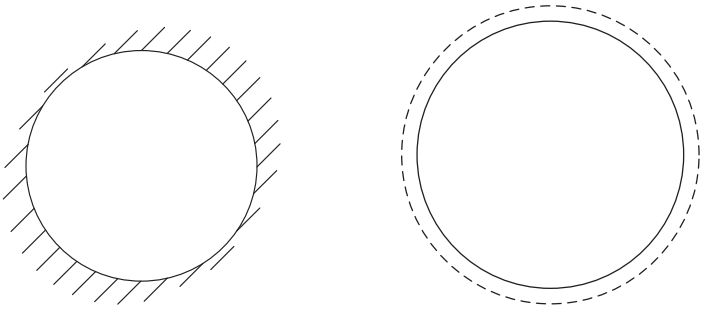

(a) Clamped circular plate (b) Simply supported circular plate

Figure 7: A circular plate of radius a subjected to a uniform transversal load q

The deflections and moment along the radius for the clamped and simply supported circular plates subjected to a uniform load are shown in Figs. 8 and 9. In the present calculation, the circular is discretized using 15 nodes, and 30 internal points are used for interpolation. The comparison with analytical results indicates that the solutions are in surprisingly good agreement for both boundary conditions.

Fig. 10 represents the relative error for the bending moment M_r along the radius for clamped circular plate with different nodes arrangements. It can be observed that the results are improved considerably with the increasing number of nodes.

4.3 Simply supported square plate under uniform load

Consider an uniformly loaded simply supported square plate (see Fig. 11). This is a case for which there is an analytical solution in the form [Timoshenko and Woinowsky-Krieger (1959)]:

$$w = \frac{16q}{\pi^6 D}\sum_{m=1,3,\cdots}^{\infty}\sum_{n=1,3,\cdots}^{\infty}\frac{\sin\frac{m\pi x}{a}\sin\frac{m\pi y}{a}}{mn\left(\frac{m^2}{a^2}+\frac{n^2}{a^2}\right)^2} \tag{82}$$

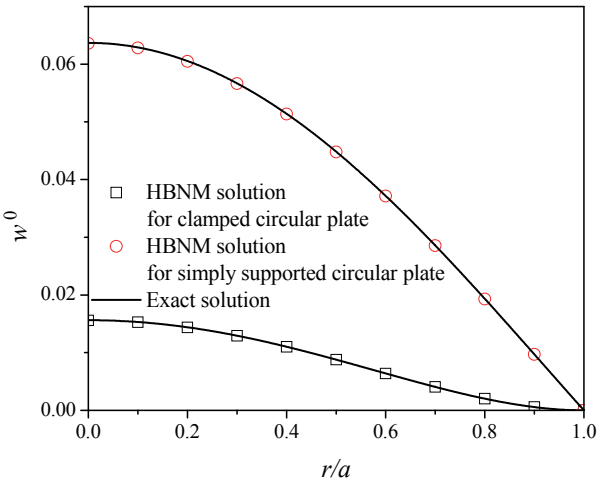

Figure 8: Deflection w along the radius ($w^0 = Dw/qa^4$)

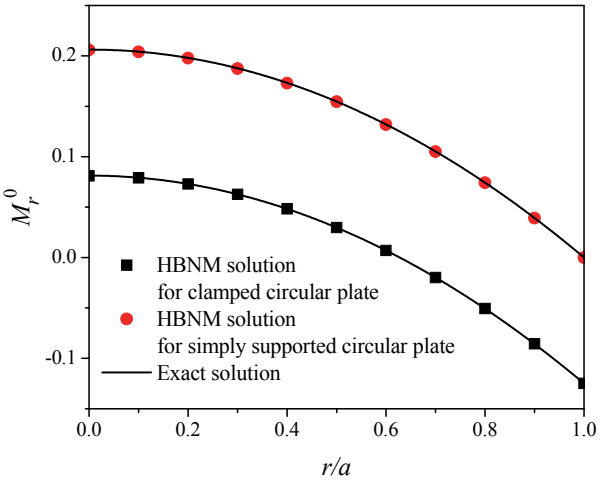

Figure 9: Bending moment M_r along the radius ($M_r^0 = M_r/qa^2$)

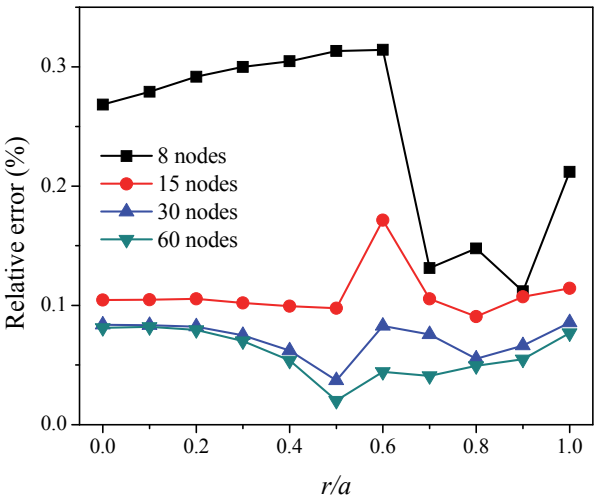

Figure 10: Relative error for the bending moment M_r along the radius for clamped circular plate

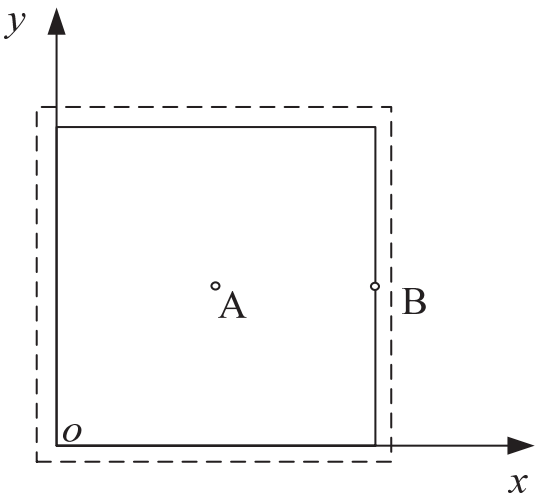

Figure 11: Simply supported square plate

The normal slope θ_n along the simply supported edge $x = 0$ is presented in Fig. 12. For the case, 10 nodes are uniformly distributed on each segment of the boundary and 20 additional internal points are used. A good agreement between the present solution and the analytical solution has been achieved. It can be seen that the numerical solutions are accurate even if near the boundary, and the 'boundary layer effect' vanishes by using this method.

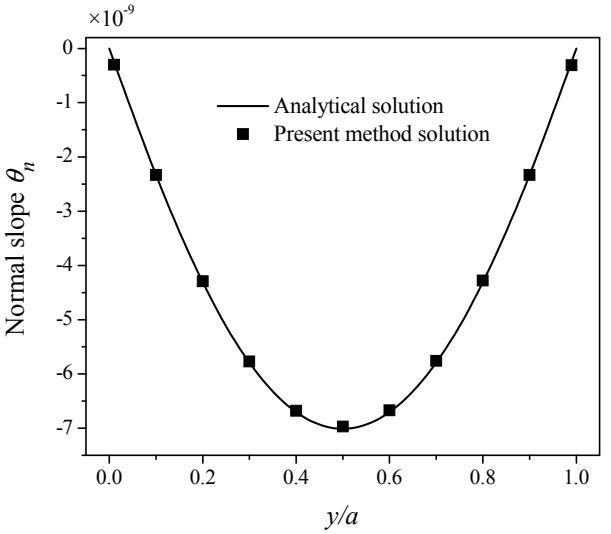

Figure 12: Normal slope θ_n along the simply supported edge $x = 0$

To study the influence of internal points, different number of internal points is used. In Fig. 13, the relative error of the bending moment M_{xx}on $y = 0.5$ is represented with different number of internal points. It shows that the more the points are arranged in the domain, the more accurate solution can be obtained.

4.4 Clamped square plate under uniform load

A square plate subjected to a uniform distributed load with all edges clamped (see Fig. 14) is analyzed to demonstrate the versatility of the present method. In the present calculation, 8 nodes are uniformly distributed on each edge; 5, 10, 20 and 40 points are taken in the domain as internal nodes. Table 2 provides results of the present method for the central deflection and some important bending moments. It can be seen from this table that the present results are in excellent agreement, contrast with those obtained by Costa (1986) using BEM and the results solved by

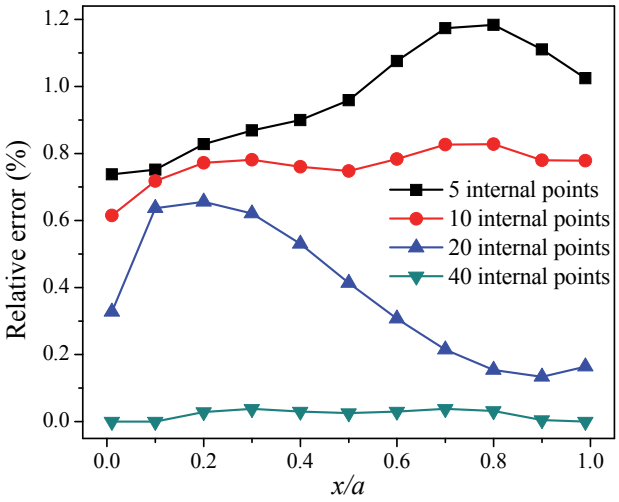

Figure 13: Relative error of the bending moment M_{xx}on $y = 0.5$ for simply supported square plate

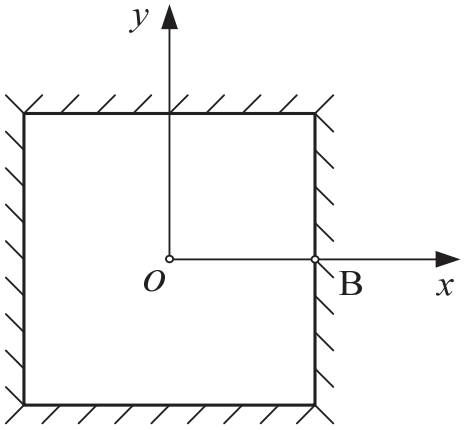

Figure 14: A square plate with all edges clamped

FEM using the commercial package ANSYS, in which the domain is discretized into 400 elements.

The deflections w along OB obtained by the present method and analytical solution [Timoshenko and Woinowsky-Krieger (1959)] are shown in Fig. 15. It shows

Table 2: Deflections and bending moments in a uniformly loaded square plate with all edges clamped

Method		Deflection at the center ($\times D/qa^4$)	Bending moment at the center ($\times 1/qa^2$)	Bending moment at half of the edge ($\times 1/qa^2$)
Present method	$L=5$	0.001255	0.022708	-0.050714
	$L=10$	0.001258	0.022751	-0.050737
	$L=20$	0.001263	0.022851	-0.051138
	$L=40$	0.001266	0.022922	-0.051371
FEM		0.001270	0.022603	-0.040820
BEM [Costa (1986)]		0.001255	0.02282	-0.05140
Analytical result		0.001265	0.022925	-0.051334

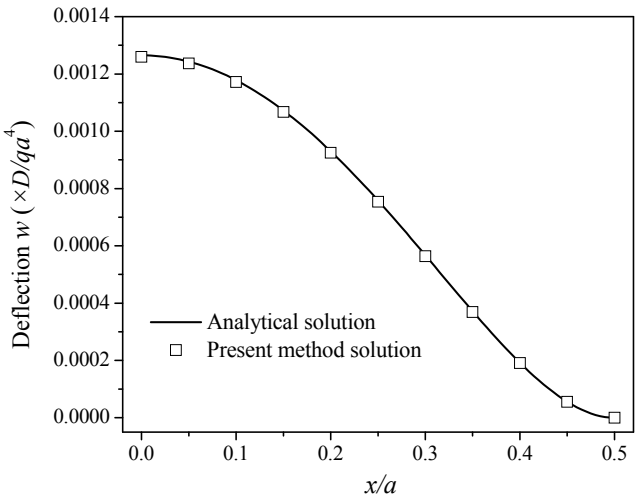

Figure 15: Deflection w along OB

that they agree well with each other. Compared with FEM and BEM, the present method has higher accuracy and requires less computation effort.

4.5 Simply supported square plate under sinusoidal load

For a simply supported square plate (see Fig. 11), we assume that the load distributed over the surface of the plate is given by the expression

$$p = q \sin \frac{\pi x}{a} \sin \frac{\pi y}{a} \tag{83}$$

in which q represents the intensity of the load at the center of the plate.

The analytical solution for this problem is [Timoshenko and Woinowsky-Krieger (1959)]:

$$w = \frac{q}{\pi^4 D \left(\frac{1}{a^2} + \frac{1}{a^2}\right)^2} \sin \frac{\pi x}{a} \sin \frac{\pi y}{a} \tag{84}$$

For the case, 10 nodes are uniformly distributed on each segment of the boundary and 60 additional internal points are used.

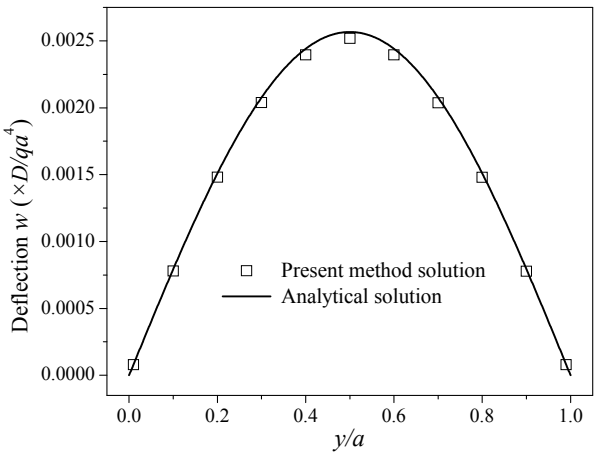

Figure 16: Deflection w of the simply supported square plate under sinusoidal load along centerline x=0.5a

In Fig. 16, 17 and 18, the numerical results for the deflection, the bending moments and the shear forces are plotted against the analytical solution. Even though the lateral load is the complicated trigonometric function, the accuracy of both the bending moments and the shear forces is great.

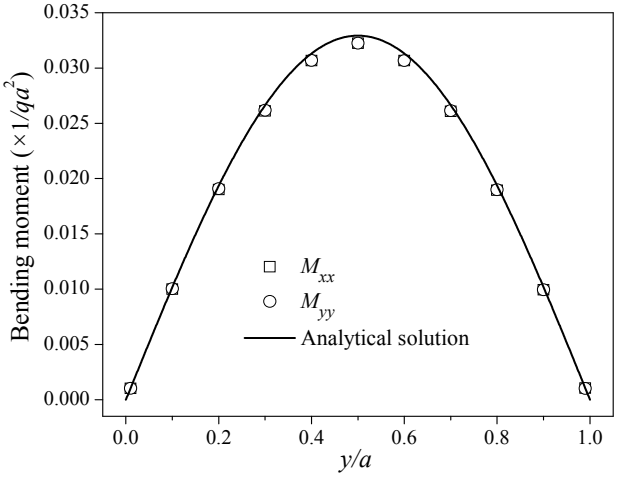

Figure 17: Bending moments of the simply supported square plate under sinusoidal load along centerline x=0.5a

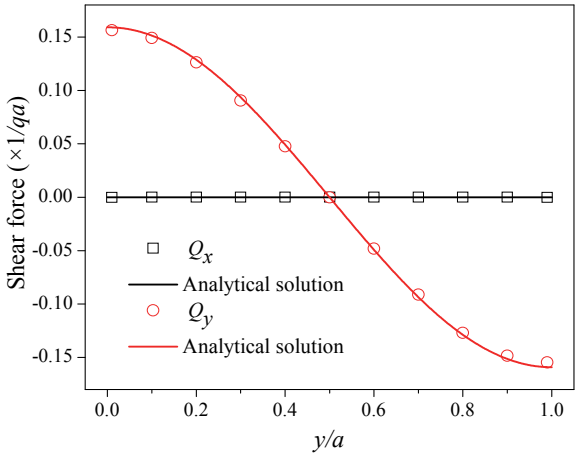

Figure 18: Shear forces of the simply supported square plate under sinusoidal load along centerline x=0.5a

5 Conclusions

In this work, a truly boundary type meshless method for the analysis of bending of thin homogeneous plates has been presented. This meshless method combines HBNM and DRM, where HBNM is used to solve the complementary solution of

the homogeneous biharmonic equation and DRM is employed to deal with the inhomogeneous term and obtain the particular solution. Detailed formulations for solving such problems are developed. The main advantages of the proposed technique are its meshless character and dimensionality reduction. These features make the approach simple to implement and, consequently, computationally efficient.

The formulation has been assessed from the comparison of the results obtained by the present method on a series of Kirchhoff plates with the analytical solution and results of other numerical methods. The results show that the present approach is sufficiently accurate and effective. Furthermore, the influences of some computation parameters are studied. It is observed that the accuracy can be improved by increasing the number of internal points.

There are many aspects of the use of the present method for Kirchhoff plates to be addressed and further developed. In the near future, efforts will be directed on the dynamic analysis of thin elastic plates by employing the present approach.

Acknowledgement: This work is supported by the "Hundred Talents Program" of the Chinese Academy of Sciences, the Scientific Research Foundation for the Returned Overseas Chinese Scholars of State Education Ministry and the Natural Science Foundation of China (No. 50808090).

References

Altiero, N.J.; Sikarskie, D.L. (1978): A boundary integral method applied to plates of arbitrary plane forms. *Computers & Structures*, vol. 9, pp. 163-168.

Atluri, S.N. (2004): *The Meshless Method (MLPG) for Domain & BIE Discretizations*. Tech Science Press, Forsyth, GA, USA.

Atluri, S.N.; Shen, S. (2002a): *The Meshless Local Petrov-Galerkin (MLPG) Method*. Tech Science Press, Forsyth, GA, USA.

Atluri, S.N.; Shen, S. (2002b): The meshless local Petrov-Galerkin (MLPG) method: A simple & less-costly alternative to the finite element and boundary element methods. *CMES: Computer Modeling in Engineering & Sciences*, vol. 3, no. 1, pp. 11-51.

Atluri, S.N.; Sladek, J.; Sladek, V.; Zhu, T. (2000): The local boundary integral equation (LBIE) and it's meshless implementation for linear elasticity. *Computational Mechanics*, vol. 25, pp. 180-198.

Atluri, S.N.; Zhu, T. (1998): A new meshless local Petrov-Galerkin (MLPG) approach in computational mechanics. *Computational Mechanics*, vol. 22, pp. 117-127.

Atluri, S.N.; Zhu, T.L. (2000): The meshless local Petrov-Galerkin (MLPG) approach for solving problems in elasto-statics. *Computational Mechanics*, vol. 25, pp. 169-179.

Belytschko, T.; Krogauz, Y.; Organ, D.; Fleming, M.; Krysl, P. (1996): Meshless methods: an overview and recent developments. *Computer Methods in Applied Mechanics and Engineering*, vol. 139, pp. 3-47.

Belytschko, T.; Lu, Y.Y.; Gu, L. (1994): Element-free Galerkin methods. *International Journal for Numerical Methods in Engineering*, vol. 37, pp. 229-256.

Chen, Wen; Fu, Zhuo-Jia Fu; Qin, Qing-Hua (2009): Boundary Particle Method with High-Order Trefftz Functions. *CMC: Computers, Materials, & Continua*, vol. 13, no. 3, pp. 201-218.

Costa, J.A. (1986): *The boundary element method applied to plate problems*. PhD thesis, Southampton University, Southampton, UK.

Frangi, A.; Bonnet, M. (1998): A Galerkin symmetric and direct BIE method for Kirchhoff elastic plates: formulation and implementation. *International Journal for Numerical Methods in Engineering*, vol. 41, pp. 337-369.

Fu, Z.J.; Chen, W. (2009): A truly boundary-only meshfree method applied to Kirchhoff plate bending problems. *Advances in Applied Mathematics and Mechanics*, vol. 1, no. 3, pp. 341-352.

Gu, Y.T.; Liu, G.R. (2001): A meshless local Petrov-Galerkin (MLPG) formulation for static and free vibration analysis of thin plates. *CMES: Computer Modeling in Engineering & Sciences*, vol. 2, no. 4, pp. 463-476.

Jaswon, M.A.; Maiti, M. (1968): An integral equation formulation of plate bending problems. *Journal of Engineering Mathematics*, vol. 2, n. 1, pp. 83-93.

Kitipornchai, S.; Liew, K.M.; Cheng, Y. (2005): A boundary element-free method (BEFM) for three-dimensional elasticity problems. *Computational Mechanics*, vol. 36, pp. 13-20.

Kothnur, V.S.; Mukherjee, S.; Mukherjee, Y.X. (1999): Two-dimensional linear elasticity by the boundary node method. *International Journal of Solids and Structures*, vol. 36, pp. 1129-1147.

Lancaster, P.; Salkauskas, K. (1981): Surfaces generated by moving least squares methods. *Mathematics in Computation*, vol. 37, no. 155, pp. 141-158.

Leitao, V.M.A. (2001): A meshless method for Kirchhoff plate bending problems. *International Journal for Numerical Methods in Engineering*, vol. 52, pp. 1107-1130.

Leonetti, L.; Mazza, M.; Aristodemo, M. (2009): A symmetric boundary element model for the analysis of Kirchhoff plates. *Engineering Analysis with Bound-*

ary Elements, vol. 33, pp. 1-11.

Li, X.L.; Zhu, J.L. (2009): A Galerkin boundary node method for two-dimensional linear elasticity. *CMES: Computer Modeling in Engineering & Sciences*, vol. 45, no. 1, pp. 1-29.

Li, X.L.; Zhu, J.L. (2011): Galerkin boundary node method for exterior Neumann problems. *Journal of Computational Mathematics*, vol. 29, no. 3, pp. 243-260.

Liew, K.M.; Cheng, Y.; Kitipornchai, S. (2006): Boundary element-free method (BEFM) and its application to two-dimensional elasticity problems. *International Journal for Numerical Methods in Engineering*, vol. 65, pp. 1310-1332.

Liu, G.R.; Gu, Y.T. (2001): A point interpolation method for two-dimensional solid. *International Journal for Numerical Methods in Engineering*, vol. 50, pp. 937-951.

Long, S.Y.; Atluri, S.N. (2002): A meshless local Petrov-Galerkin method for solving the bending problem of a thin plate. *CMES: Computer Modeling in Engineering & Sciences*, vol. 3, no. 1, pp. 53-63.

Miao, Y.; Wang Q.; Liao, B.H.; Zheng, J.J. (2009): A dual hybrid boundary node method for 2D elastodynamics problems. *CMES: Computer Modeling in Engineering & Sciences*, vol. 53, no. 1, pp. 1-22.

Miao, Y.; Wang Y.H.; Yu, F. (2005): Development of hybrid boundary node method in two-dimensional elasticity. *Engineering Analysis with Boundary Elements*, vol. 29, pp. 703-712.

Mukherjee, Y.X.; Mukherjee, S. (1997a): The boundary node method for potential problems. *International Journal for Numerical Methods in Engineering*, vol. 40, pp. 797-815.

Mukherjee, Y.X.; Mukherjee, S. (1997b): On boundary conditions in the element-free Galerkin method. *Computational Mechanics*, vol. 19, pp. 264-270.

Paris, F.; Leon, S.D. (1986): Simply supported plates by the boundary integral equation method. *International Journal of Solids and Structures*, vol. 23, pp. 173-191.

Paris, F.; Leon, S.D. (1987): Boundary element method applied to the analysis of thin plates. *Computers & Structures*, vol. 25, pp. 225-233.

Patridge, P.W.; Brebbia, C.A.; Wroble, L.W. (1992): *The Dual Reciprocity Boundary Element Method*. Computational Mechanics Publication, Southampton, UK.

Sladek, J.; Sladek, V.; Mang, H.A. (2002): Meshless formulations for simply supported and clamped plate problems. *International Journal for Numerical Methods in Engineering*, vol. 55, pp. 359-375.

Stern, M. (1979): A general boundary integral formulation for the numerical solution of plate bending problems. *International Journal of Solids and Structures*, vol. 15, pp. 769-782.

Timoshenko, S.; Woinowsky-Krieger, S. (1959): *Theory of Plates and Shells*. 2nd ed. McGraw-Hill, New York, USA.

Wang, J.G.; Liu, G.R. (2002): A point interpolation method based on radial basis functions. *International Journal for Numerical Methods in Engineering*, vol. 54, pp. 1623-1648.

Yan, F.; Wang, Y.H.; Miao, Y.; Cheung, Y.K. (2009): Dual reciprocity hybrid boundary node method for free vibration analysis. *Journal of Sound and Vibration*, vol. 321, pp. 1036-1057.

Yun, B.I.; Ang, W.T. (2010): A Dual-Reciprocity Boundary Element Simulation of Axisymmetric Dual-Phase-Lag Heat Conduction in Nonhomogeneous Media. *CMES: Computer Modeling in Engineering & Sciences*, vol. 65, no. 3, pp. 217-244.

Zhang, J.M.; Yao, Z.H. (2001): Meshless regular hybrid boundary node method. *CMES: Computer Modeling in Engineering & Sciences*, vol. 2, no. 3, pp. 307-318.

Zhang, J.M.; Yao, Z.H. (2004): The regular hybrid boundary node method for 2D linear elasticity. *Engineering Analysis with Boundary Elements*, vol. 27, pp. 259-268.

Zhang, J.M.; Yao, Z.H.; Li, H. (2002): A hybrid boundary node method. *International Journal for Numerical Methods in Engineering*, vol. 53, pp. 751-763.

Zhu, T.; Atluri, S.N. (1998): A modified collocation & penalty formulation for enforcing the essential boundary conditions in the element free Galerkin method. *Computational Mechanics*, vol. 21, pp. 211-222.

Zhu, T.; Zhang, J.D.; Atluri, S.N. (1998): A local boundary integral equation (LBIE) method in computational mechanics, and a meshless discretization approach. *Computational Mechanics*, vol. 21, pp. 223-235.

Zienkiewicz, O.C. (1977): *Finite Element Method*. McGraw-Hill, New York, USA.